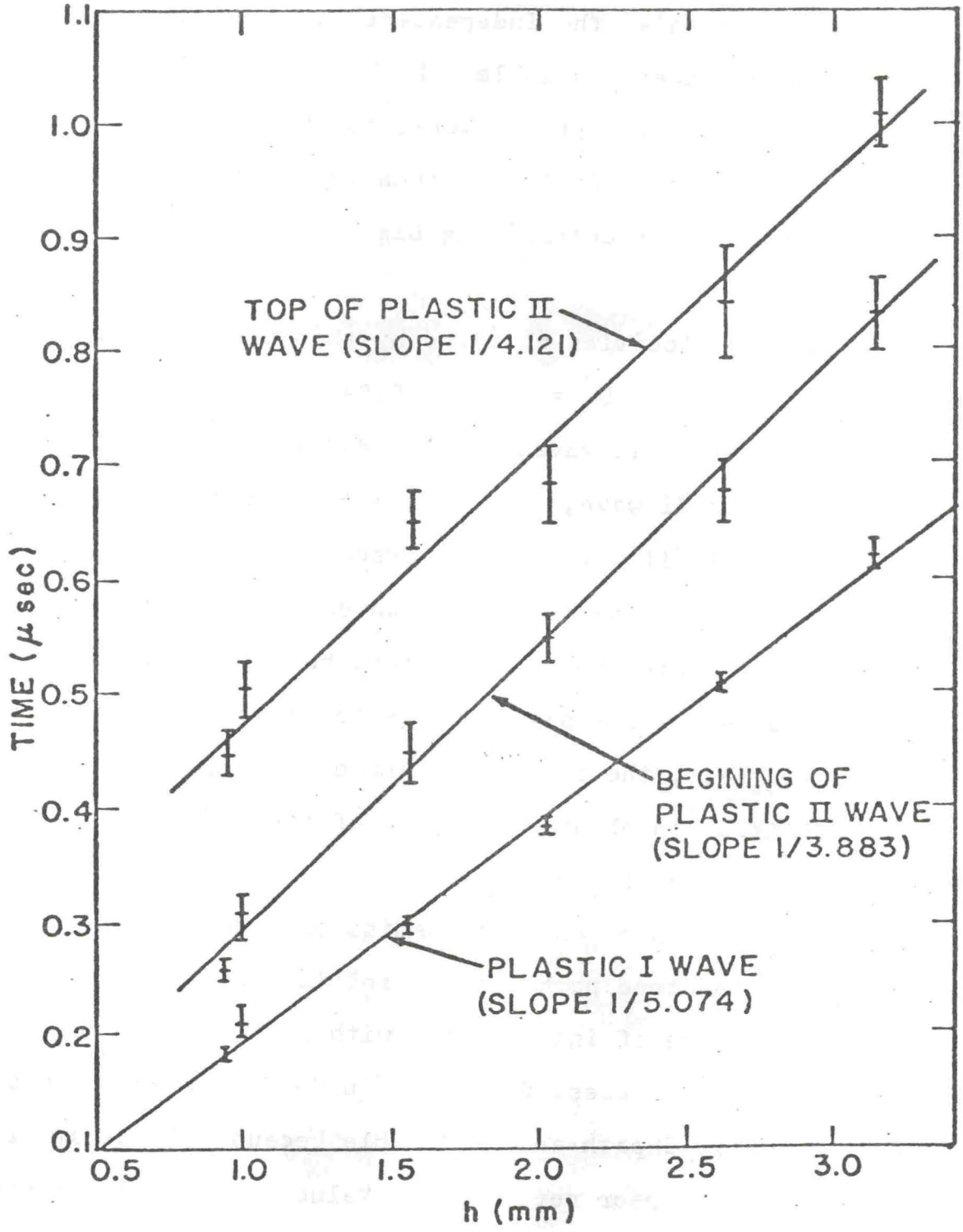

Fig. 4.5.--Shock wave arrival times at free surfaces.

The arrival times were fit by least squares to straight lines, with arrival time taken as the independent variable and sample thickness as the dependent variable. Each arrival time was assigned a weighting factor proportional to the inverse square of its error. Differences in final stress reached in the iron samples were ignored when determining Lagrangian velocity of the plastic II shock wave.

Lagrangian velocities obtained by this procedure are:

plastic I wave, $U_2' = 5.074 \pm 0.045$ mm/μsec;

beginning of plastic II wave, $U_{3B}' = 3.883 \pm 0.138$ mm/μsec;

top of plastic II wave, $U_{3T}' = 4.121 \pm 0.235$ mm/μsec.

The beginning plastic II wave path intersects the $h=0$ plane at $t = 0.23 \pm 0.017$ sec. The top of the wave front appears to propagate slightly faster than the bottom, but errors in the velocities do not allow any significance to be assigned to this observation. In fact, the error bars are of such large magnitude that no conclusion about steadiness of the wave front can be drawn from the data of Fig. 4.5.

The h-t plots of shock transmission times in Fig. 4.5 do not represent the true paths of the initial forward-facing plastic shocks because of interactions with backward-facing waves from the free surfaces, described in Section 2.2. Corrections to the plastic I path are negligible because of the small amplitude of the precursor reflection. Values of (h,t) points for the beginning of the plastic II wave, corrected according to Eqs. (2.9) and (2.10), are shown in Fig. 4.6. The rectangles represent estimated errors for each point. The fitted line